Orbital gravitomagnetoelectric response and orbital magnetic quadrupole moment correction

Koki Shinada[*] and Robert Peters

Department of Physics, Kyoto University, Kyoto 606-8502, Japan

We propose a fully quantum-mechanical formalism for the temperature-gradient-induced orbital magneto-electric effect in systems without spatial inversion symmetry, $\mathcal{P}$, and time-reversal symmetry $\mathcal{T}$. The effect consists of two parts, i.e., an extrinsic part and an intrinsic part. We demonstrate that for the intrinsic part, a correction from the orbital magnetic quadrupole moment besides the usual Kubo formula, is necessary to avoid an unphysical divergence at zero temperature and to satisfy the Mott relation. Furthermore, we show the classification table with the magnetic point group for the intrinsic and extrinsic effects. Finally, we analyze the intrinsic part in a $\mathcal{PT}$-symmetric model exhibiting an orbital magnetization order, i.e., a loop-current order, and demonstrate the enhancement near Dirac points. We believe these results will contribute to the detection and application of orbital magnetic moments beyond spin moments.

I. INTRODUCTION

Orbital angular momentum is one of the fundamental degrees of freedom of electrons along with charge and spin. Electrons bound to a nucleus form electron clouds, characterized by the orbital angular momentum, such as *s*-wave symmetry and *p*-wave symmetry. In solids, electrons are exposed to the periodic potential created by the lattice of nuclei where some electrons are not bound anymore to a particular nucleus but can move through the lattice. These electrons can circulate in solids generating orbital magnetic moments (OMMs) and can even create a bulk magnetization, such as in loop-current order. The calculation of the OMM in solids has been a challenging theoretical problem because the angular momentum depends on the position operator that is unbounded and, thus, ill-defined in solids. This problem has been solved in the modern theory of the orbital magnetic moment [1–5].

The OMM is the cause of various phenomena. For example, the valley Hall effect has been proposed and experimentally observed as an analog to the spin Hall effect [6,7]. Furthermore, in orbitronics beyond spintronics, it has been recently explored how to manipulate and transport the OMMs [8]. Particularly, it is discussed that magnetization dynamics important in device applications can be created by orbital transports [9–16].

Besides the necessity of electrically manipulating magnetic moments to apply them in devices, there also is an ongoing fundamental interest in it. The magnetoelectric effect (ME effect) has been energetically studied in systems without spatial-inversion $\mathcal{P}$ and time-reversal symmetry $\mathcal{T}$. In the ME effect, magnetization can be induced by an electric field, or polarization can be induced by a magnetic field, and such cross correlations are attracting attention for their ability to characterize the symmetry of materials. Since its first observation in the antiferromagnet Cr_2O_3 [17–19], the ME effect has been discussed mainly for spin degrees of freedom in multiferroics [20–24]. Magnetization can also be induced by a current, which is called the Edelstein effect [25]. Of course, besides spin polarization, OMMs also generate magnetization. Thus, the orbital version of the ME effect and the Edelstein effect can be anticipated. In fact, the orbital ME effect has been discussed in topological insulators. This effect has two parts: Kubo terms and a Chern-Simons term [26–30]. Especially, the Chern-Simons term has a topological nature and yields a quantized value for the ME effect in topological insulators. Furthermore, this term introduces the axion coupling rewriting the Maxwell equation anew and paving the way for the axion electrodynamics [31]. However, the Chern-Simons term is not yet directly observed but only indirectly [32–35].

Although the orbital ME effect in topological insulators is diligently researched due to its topological property, the orbital ME effect in metals is just beginning to attract attention. The orbital Edelstein effect in metals has been theoretically discussed [36–42] and recently observed in strained MoS_2 [43,44] and twisted bilayer graphene [45,46]. In particular, twisted bilayer graphene has a large OMM resulting in a giant orbital Edelstein effect. The orbital Edelstein effect is also discussed in superconductors yielding a nondissipative response [47,48]. Furthermore, the intrinsic orbital ME effect in metals is recently formalized using semiclassical theory [49,50] or a fully quantum-mechanical analysis [51] in the Bloch basis. It has been shown that the intrinsic orbital ME effect can be used to detect $\mathcal{PT}$-symmetric orbital magnets, such as an antiferromagnetic loop current order, and it implies that the orbital ME effect is useful for the detection of higher-order multipoles, such as orbital magnetic quadrupole moments. Furthermore, the orbital ME effect is recently studied in nanoribbons of honeycomb lattices using the intra-atomic approximation [52,53].

_____
[*]shinada.koki.64w@st.kyoto-u.ac.jp

Besides electric fields, also temperature gradients can induce magnetization. The thermal version of the spin ME effect (spin gravito-ME effect) and the spin Edelstein effect are discussed in systems with spin-orbit coupling [54–58]. Usually, in theoretical calculations of thermal response functions, there are certain aspects that need special consideration. In general, when calculating the intrinsic thermal response, the Kubo formula alone is not sufficient; certain equilibrium contributions of magnetic multipoles need to be subtracted [58–60]. Otherwise, response functions diverge at zero temperature, which is an unphysical behavior.

In this paper, we propose a proper calculation for the *orbital* gravito-ME response within a full quantum-mechanical calculation. First, we show in Sec. II that the second derivative of the current energy-density correlation function includes the information on the orbital gravito-ME tensor. Second, we show in Sec. III A that the intrinsic orbital gravito-ME response needs a correction from a higher-order magnetic multipole moment, an orbital magnetic quadrupole moment. Third, we derive equations for the intrinsic and extrinsic orbital gravtio-ME effects in periodic metals at finite temperature in Secs. III B–III D. In addition, we show that these equations satisfy the Mott relation, similar to the relationship between electrical conductivity and thermoelectric conductivity, and that each two parts have no unphysical divergence at zero temperature. Fourth, we show in Sec. IV A the classification table for these responses with the magnetic point group and show that the intrinsic part can be used for the detection of $\mathcal{PT}$-symmetric orders. Finally, we calculate the intrinsic part in a model of a $\mathcal{PT}$-symmetric orbital magnet with a loop-current order in Sec. IV B and demonstrate the enhancement around Dirac points.

II. FORMALIZATION

In this section, we discuss the formalization of the orbital magnetization linearly induced by a temperature gradient, which we call the orbital gravito-magnetoelectric (OGME) response in this paper. In general, it is challenging to calculate the orbital magnetization using the Bloch basis because the position operator is unbounded. However, the orbital ME tensor is known to be contained in the current-current correlation function and the current-density correlation function, providing a way to calculate the orbital ME tensor without using the position operator [29,38,51]. Here, we will see that the OGME tensor can also be extracted from a correlation function, i.e., the linear-response function of the current density induced by a temperature gradient.

Before presenting the formalization, we briefly comment on how to calculate correlation functions induced by a temperature gradient. We need to consider the temperature gradient as an external force; however, this force cannot be simply added to the microscopic Hamiltonian because it is a statistical force. Luttinger derived a method to treat the temperature gradient as a mechanical force by introducing a gravitational potential $\psi(\mathbf{r})$ [61]. He showed that the response function induced by the gradient of the gravitational potential reproduces the temperature gradient-induced response function. This gravitational potential is added to the unperturbed

Hamiltonian H_0 as

$$H_{\text{grav}} = \int d\mathbf{x}\, \psi(\mathbf{r})H_0(\mathbf{r}), \tag{1}$$

where $H_0(\mathbf{r}) = \{H_0, \delta(\mathbf{x} - \mathbf{r})\}/2$ is a Hamiltonian density. Here, we define $\{A, B\} = AB + BA$. We note that $\mathbf{r}$ is here just a coordinate and not an operator, unlike $\mathbf{x}$. In the dynamical linear-response theory, the total current density is changed by the gravitational potential with a factor $e^{-i\omega t + \delta t}$ as

$$J^i_{\mathbf{q},\omega} = \Phi^i(\mathbf{q}, \omega)\psi_{\mathbf{q}}. \tag{2}$$

$\Phi^i(\mathbf{q}, \omega)$ is the dynamical linear-response function of the current density induced by the gravitational potential, which is discussed in this paper. This correlation function can be calculated by the usual Kubo formula because the gravitational potential is just a mechanical force. Finally, we can obtain the response function induced by the spatially varying temperature by replacing $\beta\psi_{\mathbf{q}}$ with $-\beta_{\mathbf{q}}$, where β is the inverse temperature of the system, and $\beta_{\mathbf{q}}$ is the external inverse temperature including a spatial modulation.

Next, we will move on to the formalization. We will show that the second derivative of this correlation function $\Phi^{i,jk}(\omega) = \partial_{q_j q_k}\Phi^i(0, \omega)$ includes the information of the OGME tensor. $\Phi^{i,jk}(\omega)$ is symmetric for the interchange $j \leftrightarrow k$. Thus, we can decompose this function using a traceless rank-2 tensor β_{ij}, and a totally symmetric rank-3 tensor γ_{ijk} as

$$\Phi^{k,ij}(\omega) = i\varepsilon_{jkl}\beta_{il}(\omega) + i\varepsilon_{ikl}\beta_{jl}(\omega) + \omega\gamma_{ijk}(\omega), \tag{3a}$$

$$\beta_{li}(\omega) = \frac{1}{3i}\varepsilon_{ijk}\Phi^{k,lj}(\omega), \tag{3b}$$

$$\gamma_{ijk}(\omega) = \frac{1}{3\omega}[\Phi^{i,jk}(\omega) + \Phi^{j,ki}(\omega) + \Phi^{k,ij}(\omega)]. \tag{3c}$$

Here, ε_{ijk} is the completely antisymmetric tensor. Substituting Eq. (3a) into Eq. (2), we find

$$J^i_{\mathbf{q},\omega} = -i\omega\big(-iq_j Q^{Gij}_{\mathbf{q},\omega} \big) + \big(i\mathbf{q} \times \mathbf{M}^G_{\mathbf{q},\omega}\big)_i, \tag{4a}$$

$$Q^{Gij}_{\mathbf{q},\omega} = i\gamma_{ijk}(\omega)G^k_{\mathbf{q},\omega}, \tag{4b}$$

$$M^{Gi}_{\mathbf{q},\omega} = 2i\beta_{ji}(\omega)G^j_{\mathbf{q},\omega}, \tag{4c}$$

where $\mathbf{G}_{\mathbf{q},\omega} = +i\mathbf{q}\psi_{\mathbf{q},\omega}$ corresponds to a temperature gradient. $\mathbf{M}^G_{\mathbf{q},\omega}$ and $Q^{Gij}_{\mathbf{q},\omega}$ are a magnetization and an electric quadrupole moment induced by the temperature gradient $\mathbf{G}_{\mathbf{q},\omega}$. Thus, β_{ij} can be interpreted as the OGME tensor, and γ_{ijk} is a pure electric quadrupole moment induced by the temperature gradient, which cannot be included in the OGME tensor due to its total symmetric property. In this formalism, the trace of the OGME tensor is not included. Our formalism is based on the current density, and, thus, we can obtain only terms contributing to the current density. In general, the trace of the OGME tensor β_{Tr}, does not contribute to the current density because $\mathbf{J}_{\mathbf{q},\omega} \propto \mathbf{q} \times \beta_{\text{Tr}}\mathbf{q}\psi_{\mathbf{q},\omega} = 0$. In this paper, we will derive the static and uniform traceless OGME response by calculating β_{ij}.

III. DERIVATION OF THE OGME TENSOR

In this section, we give the result of the static and uniform OGME tensor in periodic systems at finite temperatures.

When we take the static and uniform limits, we take $q \to 0$ before $\omega \to 0$ because we focus on the dynamical response [62].

A. Orbital magnetic quadrupole moment correction

When we consider the response by the gravitational force, we should note that the current density is also changed by the gravitational potential. The total current density under this potential is given by

$$J(r) = [1 + \psi(r)]J_0(r), \qquad (5)$$

where $J_0(r)$ is the unperturbed current density. Thus, there are two contributions to the linear-response function induced by the gravitational force. One contribution comes from the first term in Eq. (5). This contribution originates from the change of the density matrix by the gravitational force, and it is given by the usual Kubo linear response. It brings the correlation function between the current density and the Hamiltonian density, which we call the current energy-density correlation function $\Phi^i_{JH}(q, \omega)$. Another contribution originates from the second term. This term is already linear in the gravitational potential. Thus, we need to calculate the equilibrium expectation value of the current density $J_0(r)$. This equilibrium current plays an important role in thermal responses. In fact, it is known to give an orbital (energy) magnetization correction to the Nernst conductivity and the thermal Hall conductivity, and it eliminates an unphysical divergence at zero temperature [59,60] and these conductivities satisfy the Mott relation. We will see that the equilibrium current adds a higher-order multipole correction, an orbital magnetic quadrupole moment, to the OGME tensor, in an analogy to the thermal Hall effect.

Let us discuss the contribution from the equilibrium current in more detail. In equilibrium, a bulk current is not allowed to flow. However, a local current is not forbidden. In general, a local current can be written as a local magnetization $M(r)$ using $\langle J_0(r)\rangle_0 = \nabla \times M(r)$, which is called a magnetization current. Here, $\langle O\rangle_0$ is an expectation value of an observable operator O in equilibrium. This magnetization can be derived in a thermodynamic approach [4]. In local thermodynamics, the free-energy density $F(r)$ with a nonuniform magnetic-field $B(r)$ is given by

$$dF(r) = -M^i_0(r)dB^i(r) - Q^{(m)}_{ij}(r)d[\partial_i B^j(r)] + \cdots. \quad (6)$$

This thermodynamic relation defines multipoles conjugate to the higher-order gradient of the magnetic field, where $Q^{(m)}_{ij}(r)$ is a local magnetic quadrupole moment. Using this relationship, the local magnetization $M(r)$ is determined by

$$M^i(r) = -\partial F(r)/\partial B^i(r) = M^i_0(r) - \partial_j Q^{(m)}_{ji}(r) + O(\partial^2). \qquad (7)$$

The bulk magnetization and magnetic quadrupole moment in periodic systems can be calculated using this thermodynamic definition where their formulas are applicable even in metals at finite temperatures [4,63]. This thermodynamic magnetic quadrupole moment is recently discussed in various works [63–68].

Using the local magnetization, the contribution from the second term in Eq. (5) can be rewritten as

$$
\begin{aligned}
\psi(r)\langle J_0(r)\rangle_0 &= \psi(r)\nabla \times M(r) \\
&= \nabla \times \left\{\psi(r)M_0(r) - \partial_i\left[e_j\psi(r)Q^{(m)}_{ij}(r)\right]\right\} \\
&\quad + \nabla \times \left\{[\partial_i\psi(r)]e_jQ^{(m)}_{ij}(r)\right\} \\
&\quad - \nabla\psi(r) \times \left[M_0(r) - \partial_i e_jQ^{(m)}_{ij}(r)\right]
\end{aligned}
\qquad (8)
$$

Here, e_i is a unit vector along the i direction. The first term is the gravitational potential correction to the magnetization and the magnetic quadrupole moment. The third term represents the current-density response induced by a temperature gradient where the conductivity is determined by the local magnetization. This contribution is studied in the Nernst conductivity [59,60]. The second term is the main result of this paper. This term corresponds to a magnetization induced by a temperature gradient, i.e., the gravito-ME effect. This means that the magnetic quadrupole moment should be included in the OGME tensor besides the contribution from the current energy-density correlation function as $\chi^{\mathrm{OGME}}_{ij} = 2i\beta^{JH}_{ij} + Q^{(m)}_{ij}$ [$M^i = \chi^{\mathrm{OGME}}_{ij}(\partial_j\psi)$]. We note that the trace of the magnetic quadrupole moment is indefinite due to $\nabla \times \nabla = 0$, which is included in the second term of Eq. (8) similar to the discussion on the traceless property of β_{ij}. Thus, in the following, we discuss only the traceless part of this correction.

The magnetic quadrupole moment correction is also studied in the *spin* gravito-ME effect, where the *spin* magnetic quadrupole moment contributes to the response tensor [58]. With the gravitational potential, the spin density also changes as $[1 + \psi(r)]s(r)$ where the second term gives the contribution from the spin magnetic quadrupole moment. Our equation, on the other hand, includes the *orbital* magnetic quadrupole moment.

B. Current energy-density correlation function in periodic systems

We have shown above that we need to calculate the current energy-density correlation function and the magnetic quadrupole moment to obtain the OGME tensor. In the following, we will derive the OGME tensor in periodic systems described by a Bloch Hamiltonian.

First, we will derive the current energy-density correlation function. The Hamiltonian used in this paper is

$$H_0 = \frac{p^2}{2m} + V(x) + \frac{1}{4m^2}\left(\frac{\partial V(x)}{\partial x} \times p\right) \cdot \sigma. \qquad (9)$$

Here, m is the electron mass, $V(x)$ is a periodic potential, and σ is the vector of the Pauli matrices. The third term represents the spin-orbit coupling. The unperturbed current operator is $J_0(r) = -e\{v_0, \delta(x - r)\}/2$ and $v_0 = i[H_0, x]$ is the velocity operator. Here, $-e(<0)$ is the charge of an electron. In this paper, we set $\hbar = k_B = 1$. Using the Kubo formula, the current energy-density correlation function is given by

$$\Phi^i_{JH}(q, \omega) = -e\sum_{mn,k} \frac{f(\epsilon_{nk+q/2}) - f(\epsilon_{mk-q/2})}{\epsilon_{nk+q/2} - \epsilon_{mk-q/2} - (\omega + i\delta)} \langle u_{mk-q/2}| v^i_k |u_{nk+q/2}\rangle \frac{\epsilon_{nk+q/2} + \epsilon_{mk-q/2}}{2} \langle u_{nk+q/2}|u_{mk-q/2}\rangle. \qquad (10)$$

We define $\epsilon_{n\mathbf{k}}$, $|u_{n\mathbf{k}}\rangle$ as an eigenenergy and eigenvector of the nth band of the Bloch Hamiltonian $H_{\mathbf{k}} = e^{-i\mathbf{k}\cdot\mathbf{x}}(H_0 - \mu N)e^{+i\mathbf{k}\cdot\mathbf{x}}$. $f(\epsilon) = 1/(e^{\beta\epsilon} + 1)$ is the Fermi distribution function, and $\mathbf{v}_{\mathbf{k}} = \partial H_{\mathbf{k}}/\partial\mathbf{k}$ is the velocity operator.

C. Intrinsic OGME tensor

After having defined the current energy-density correlation function in periodic systems, we expand the correlation function up to the second order of $\mathbf{q}$ and use the relation in Eq. (3b) to derive $\beta_{ij}^{JH}(0)$ as a contribution to the OGME tensor originating from the correlation function. In this subsection, we focus on the intrinsic part. The result for the extrinsic part will be shown and discussed in the next subsection. Details of the derivation are given in Appendix A. The intrinsic part from the correlation function $(2i\beta_{li}^{JH} = \frac{2}{3}\varepsilon_{ijk}\Phi_{JH}^{k,lj})$ is

$$
2i\beta_{li}^{JH} = -e \int_{\text{BZ}} \frac{d^3k}{(2\pi)^3} \sum_n \left(\epsilon_{n\mathbf{k}} f(\epsilon_{n\mathbf{k}}) \left\{ \frac{1}{3}\varepsilon_{ijk}\partial_k g_n^{lj} - \sum_{m(\neq n)} \frac{2}{\epsilon_{nm\mathbf{k}}} \text{Re}\left[\mathcal{A}_{nm}^l M_{mn}^i - \frac{1}{3}\delta_{li}\mathcal{A}_{nm}^j M_{mn}^j \right] \right\} \right.
$$
$$
\left. + f(\epsilon_{n\mathbf{k}}) \left\{ \frac{2}{3}\sum_{m(\neq n)} \text{Re}\left[\mathcal{A}_{nm}^l M_{mn}^i \right] - \frac{1}{12}\varepsilon_{ijk}\partial_j v_n^{kl} \right\} \right). \tag{11}
$$

We use the notation $\partial_i = \partial/\partial k_i$, $\epsilon_{nm\mathbf{k}} = \epsilon_{n\mathbf{k}} - \epsilon_{m\mathbf{k}}$, and $v_n^{ij} = \langle u_{n\mathbf{k}}| \partial^2 H_{\mathbf{k}}/\partial k_i \partial k_j |u_{n\mathbf{k}}\rangle$. This equation includes several geometric quantities. First, $\mathcal{A}_{nm}^i = i \langle u_{n\mathbf{k}}|\partial_i u_{m\mathbf{k}}\rangle$ is the Berry connection. Second, $g_n^{ij} = \sum_{m(\neq n)} \text{Re}[\mathcal{A}_{nm}^i \mathcal{A}_{mn}^j]$ is the quantum metric measuring the distance of two states on the Brillouin zone [69,70]. It has been shown that the quantum metric appears in several quantities, such as the conductivity [71], the electric quadrupole moment [72], the superfluid weight [73], the nonlinear response [30,74–77], the nonreciprocal directional dichroism [78], and the orbital ME effect [49–51]. Third, $\mathbf{M}_{mn} = \sum_{l(\neq n)} \mathbf{V}_{ml,n} \times \mathcal{A}_{ln}$ ($\mathbf{V}_{ml,n} = (\mathbf{v}_{\mathbf{k}}^{ml} + \nabla\epsilon_{n\mathbf{k}}\delta_{ml})/2$ and $\mathbf{v}_{\mathbf{k}}^{ml} = \langle u_{m\mathbf{k}}| \mathbf{v}_{\mathbf{k}} |u_{l\mathbf{k}}\rangle$) corresponds to the product of the velocity and the position; thus, it corresponds to an off-diagonal orbital magnetic moment.

The orbital magnetic quadrupole moment in periodic systems has already been derived using the thermodynamic approach [63,65]. We reproduce it using our model and obtain (We only consider the traceless part.)

$$
Q_{li}^{(m)} = -e \int_{\text{BZ}} \frac{d^3k}{(2\pi)^3} \sum_n \left(-g(\epsilon_{n\mathbf{k}}) \left\{ \frac{1}{3}\varepsilon_{ijk}\partial_k g_n^{lj} - \sum_{m(\neq n)} \frac{2}{\epsilon_{nm\mathbf{k}}} \text{Re}\left[\mathcal{A}_{nm}^l M_{mn}^i - \frac{1}{3}\delta_{li}\mathcal{A}_{nm}^j M_{mn}^j \right] \right\} \right.
$$
$$
\left. - f(\epsilon_{n\mathbf{k}}) \left\{ \frac{2}{3}\sum_{m(\neq n)} \text{Re}\left[\mathcal{A}_{nm}^l M_{mn}^i \right] - \frac{1}{12}\varepsilon_{ijk}\partial_j v_n^{kl} \right\} \right). \tag{12}
$$

Here, $g(\epsilon) = -\beta^{-1} \ln(1 + e^{-\beta\epsilon})$ is the grand potential density. This equation is identical to the equations in Refs. [63,65].

Finally, combining Eqs. (11) and (12), the actual total intrinsic OGME tensor χ_{ij}^{iOGME} [$M^i = \chi_{ji}^{\text{iOGME}}(-\partial_j T)$] using the correspondence $\partial_i \psi \to \partial_i T/T$ is

$$
\chi_{ij}^{\text{iOGME}} = -\left(2i\beta_{ij}^{JH} + Q_{ij}^{(m)}\right)/T = e \int_{\text{BZ}} \frac{d^3k}{(2\pi)^3} \sum_n s(\epsilon_{n\mathbf{k}}) \left(\frac{1}{3}\varepsilon_{klj}\partial_l g_{n\mathbf{k}}^{ik} - \sum_{m(\neq n)} \frac{2}{\epsilon_{nm\mathbf{k}}} \text{Re}\left[\mathcal{A}_{nm}^i M_{mn}^j - \frac{1}{3}\delta_{ij}\mathcal{A}_{nm}^l M_{mn}^l \right] \right). \tag{13}
$$

In this calculation, we can see that terms proportional to the Fermi distribution function in Eqs. (11) and (12) cancel each other. This equation is the main result of this paper. $s(\epsilon) = \epsilon f(\epsilon)/T - g(\epsilon)/T$ is an entropy density. The OGME tensor is very similar to the orbital ME tensor (see Ref. [51]). The only difference is that the entropy density $s(\epsilon_{n\mathbf{k}})$ in the OGME tensor is replaced by the Fermi distribution function $f(\epsilon_{n\mathbf{k}})$ in the orbital ME tensor. It is natural that the entropy density appears in the thermal response. Because the entropy density becomes zero at zero temperature, the OGME tensor approaches zero with decreasing temperature and has no unphysical divergence, which used to be a problem for the thermal Hall effect. In addition, the similarity to the orbital ME tensor leads to the following relation (see Appendix B for the details),

$$
\chi_{ij}^{\text{iOGME}}(\mu, T) = \int d\epsilon \frac{(\epsilon - \mu)}{eT} \frac{\partial f(\epsilon - \mu)}{\partial \epsilon} \chi_{ij}^{\text{iOME}}(\epsilon, T = 0)
$$
$$
\simeq \frac{-\pi^2 T}{3e} \frac{\partial \chi_{ij}^{\text{OME}}(\mu, 0)}{\partial \mu} \quad (T \to 0). \tag{14}
$$

Here, $\chi_{ij}^{\text{iOME}}(\mu, T = 0)$ is the intrinsic orbital ME tensor at the chemical potential μ and zero temperature. This equation is known as the Mott relation, which was first introduced as a relation between electric conductivity and thermoelectric conductivity [79]. Now, this relation is known to hold for various responses, such as the quantum anomalous Hall current [80], the conserved spin current [81], the spin ME effect

[58], and more general cases [82]. Thus, a similar relation is valid for the orbital magnetization induced by an electric field and a temperature gradient. The second line of this equation shows the behavior at low temperatures demonstrating that the OGME tensor scales T linear at low temperatures.

We note that our formula is gauge invariant because it is only written by the off-diagonal Berry connection and the velocity, which are gauge invariant. Finally, we comment on previous works. The intrinsic OGME tensor has been studied using the semiclassical theory in Refs. [49,50]. There is a small difference to our formula, i.e., the 1/3 factor in Eq. (13) is replaced by 1/2 in Refs. [49,50].

D. Extrinsic OGME tensor

In this subsection, we will discuss the extrinsic part of the OGME tensor. Using the relation in Eq. (3b), the extrinsic part $\chi_{ij}^{\mathrm{eOGME}}$ [$M^i = \chi_{ji}^{\mathrm{eOGME}}(-\partial_j T)$] is (see Appendix A for a detailed derivation),

$$
\begin{aligned}
\chi_{ij}^{\mathrm{eOGME}} &= -2i\beta_{ij}^{JH}/T \\
&= \frac{e}{\delta T} \int_{\mathrm{BZ}} \frac{d^3k}{(2\pi)^3} \sum_n \epsilon_{nk} \frac{\partial f(\epsilon_{nk})}{\partial \epsilon_{nk}} \\
&\quad \times \left\{ \frac{\partial \epsilon_{nk}}{\partial k_i} m_{nk}^j - \frac{1}{3}\delta_{ij}\frac{\partial \epsilon_{nk}}{\partial k_l} m_{nk}^l \right\}.
\end{aligned} \tag{15}
$$

Here, $m_{nk} = \mathrm{Im}[\langle \nabla u_{nk}| \times (\epsilon_{nk} - H_k)|\nabla u_{nk}\rangle]/2$ is the OMM, and δ is an adiabatic factor corresponding to the inverse of the dissipation strength. Due to δ, the extrinsic part has a Drude-like singularity. Furthermore, it originates at the Fermi surface.

Here, we shortly comment on the time-reversal symmetry in the case of the extrinsic OGME tensor. The integrand in this equation is even against the time-reversal operation because the OMM m_{nk} and the Bloch wave-vector k are odd. As mentioned above, the (gravito-) ME effect needs time-reversal symmetry breaking. In the case of the extrinsic OGME, the change in the distribution function together with dissipation effectively break time-reversal symmetry. Thus, the Hamiltonian of the system does not need to break time-reversal symmetry. For this reason, the extrinsic part is better interpreted as a current inducing the magnetization ($M^i = \chi_{ji}J^j$), which is usually called the Edelstein effect.

The extrinsic part also satisfies the Mott relation (see Appendix B for details),

$$
\begin{aligned}
\chi_{ij}^{\mathrm{eOGME}}(\mu, T) &= \int d\epsilon \frac{(\epsilon - \mu)}{eT} \frac{\partial f(\epsilon - \mu)}{\partial \epsilon} \chi_{ij}^{\mathrm{eOME}} \quad (\epsilon, T = 0) \\
&\simeq \frac{-\pi^2 T}{3e} \frac{\partial \chi_{ij}^{\mathrm{eOME}}(\mu, 0)}{\partial \mu} \quad (T \to 0).
\end{aligned} \tag{16}
$$

Here, $\chi_{ij}^{\mathrm{eOME}}(\epsilon, T = 0)$ is the extrinsic orbital ME tensor at the chemical potential μ and zero temperature.

IV. SYMMETRY ANALYSIS AND MODEL CALCULATION

A. Magnetic point-group symmetry analysis

In the above discussion, we have shown that there are two parts to the OGME response, an extrinsic part and an intrinsic

part. In general, the breaking of both the time-reversal symmetry and the inversion symmetry is needed for the (gravito-) ME response. Thus, we need to use magnetic point groups (MPG) to analyze whether the responses can exist. As explained above, the extrinsic part is a dissipation effect that does not need a time-reversal symmetry breaking of the Hamiltonian. Due to the difference in how both parts change with respect to the time-reversal symmetry, the conditions for their appearance are different. In fact, the extrinsic part is an axial and time-reversal-even rank-2 tensor, and the intrinsic part is an axial and time-reversal-odd rank-2 tensor. The classification table is created according to their symmetries and shown in Table I.

Let us make some comments on the table. When the system obeys $\mathcal{PT}$ symmetry, the product of inversion symmetry $\mathcal{P}$ and time-reversal symmetry $\mathcal{T}$, and the orbital magnetic moment m_{nk} vanishes. Thus, the extrinsic part cannot appear. Most of the symmetry groups generating only the intrinsic part obey $\mathcal{PT}$ symmetry; however, three groups without $\mathcal{PT}$ symmetry ($\bar{6}'$, $\bar{6}'m'2$, $\bar{6}'m'2'$) also only have an intrinsic response, as shown in Table I. There are 21 $\mathcal{PT}$-symmetric groups out of 122 magnetic point groups. Thus, Table I shows that the intrinsic response is sensitive for detecting many of the $\mathcal{PT}$-symmetric MPGs. On the other hand, when the system fulfills $\mathcal{T}$ symmetry, the intrinsic part is forbidden.

Let us now comment on the classification of the intrinsic part. We show in Table I that there are 53 groups with a finite intrinsic part [Eq. (13)]. However, there are 58 groups allowing for the intrinsic ME effect, in general. As mentioned above, our equation of the intrinsic part [Eq. (13)] is traceless. In other words, the monopole term is not included. In general, the monopole term can exist and, e.g., corresponds to the Chern-Simons term. This monopole term is allowed in the remaining five groups (23, $m'\bar{3}'$, 432, $\bar{4}'3m'$, and; $m'\bar{3}'m'$). These five groups are written in the square brackets ([ ]) in Table I.

Moreover, we comment on the relation with the nonlinear (second-order) Hall effect. In general, the nonlinear Hall effect consists of an extrinsic Hall effect induced by the Berry curvature dipole [86] and an intrinsic Hall effect [30,74,87,88]. The extrinsic part is written by an axial and time-reversal-even rank-2 tensor, and the intrinsic part is written by an axial and time-reversal-odd rank-2 tensor. Thus, the conditions for the appearance are identical to the extrinsic part and the intrinsic part of the orbital (gravito-) ME effect [87]. However, there is a small difference between the orbital (gravito-) ME effect and the nonlinear Hall effect due to symmetry-unrelated constraints. The extrinsic nonlinear Hall effect is traceless due to $\nabla \cdot \mathbf{\Omega}_{nk} = 0$. Thus, the extrinsic nonlinear Hall effect vanishes for the groups in the square brackets ([ ]) in Table I. However, the extrinsic orbital (gravito-) ME effect can appear because the orbital magnetic moment $\nabla \cdot m_{nk}$ is not necessarily zero [37,38]. Furthermore, the intrinsic nonlinear Hall effect is zero in insulators; however, the intrinsic orbital (gravito-) ME effect is generally finite in insulators. These facts show that the orbital (gravito-) ME effect occurs together with the nonlinear Hall response. However, the orbital (gravito-) ME effect can occur in systems where the nonlinear Hall effect is absent due to symmetry-unrelated constraints and, thus, might sometimes be more

TABLE I. Table classifying whether the extrinsic part and the intrinsic part of the orbital (gravito-) magnetoelectric response can be finite in a (MPG. The results are obtained using MTENSOR in the Bilbao Crystallographic Server [83–85]. corresponds to a finite response, whereas, - corresponds to a vanishing response. Groups not included in this table do not produce either response. The symbols $\mathcal{P}$ and $\mathcal{T}$ correspond to the inversion symmetry and the time-reversal symmetry. $\mathcal{PT}$ represents the operation of the product of $\mathcal{P}$ and $\mathcal{T}$.

	MPG	Intrinsic	Extrinsic
$(\mathcal{PT}\bigcirc, \mathcal{T}\times)$	$\bar{1}'$, $2'/m$, $2/m'$, $m'mm$, $m'm'm'$, $4/m'$, $4'/m'$, $4/m'mm$, $4'/m'm'm$, $4/m'm'm'$, $\bar{3}'$, $\bar{3}'m$, $\bar{3}'m'$, $6/m'$, $6/m'mm$, $6/m'm'm'$	$\checkmark$	$-$
$(\mathcal{PT}\times, \mathcal{T}\times)$	$\bar{6}'$, $\bar{6}'m'2$, $\bar{6}'m2'$, $[m'\bar{3}'$, $\bar{4}'3m'$, $m'\bar{3}'m']$		
$(\mathcal{PT}\times, \mathcal{T}\times)$	1, 2, $2'$, m, m', 222, $2'2'2$, $mm2$, $m'm2'$, $m'm'2$, 4, $4'$, $\bar{4}$, $\bar{4}'$, 422, $4'22'$, $42'2'$, $4mm$, $4'm'm$, $4m'm'$, $\bar{4}2m$, $\bar{4}'2'm$, $\bar{4}'2m'$, $\bar{4}2'm'$, 3, 32, $32'$, $3m$, $3m'$, 6, 622, $62'2'$, $6mm$, $6m'm'$, $[23, 432]$	$\checkmark$	$\checkmark$
$(\mathcal{PT}\times, \mathcal{T}\bigcirc)$	$11'$, $21'$, $m1'$, $2221'$, $mm21'$, $41'$, $\bar{4}1'$, $4221'$, $4mm1'$, $\bar{4}2m1'$, $31'$, $321'$, $3m1'$, $61'$, $6221'$, $6mm1'$, $[231', 4321']$	$-$	$\checkmark$
$(\mathcal{PT}\times, \mathcal{T}\times)$	$6'$, $6'22'$, $6'mm'$, $[4'32']$		

suitable as a probe. Finally, we note that a relation between the nonlinear Hall effect and the spin ME effect has been recently discussed in a ferrotoroidic metal UNi$_4$B [89,90].

B. Model calculation

In this subsection, we calculate the intrinsic OGME tensor in a specific model. In the previous subsection, we have shown the list classifying allowed groups for the OGME tensor. Groups in the top row in Table I are useful to detect the intrinsic OGME response because the extrinsic part vanishes.

Furthermore, orbital magnetization does, in general, not need spin degrees of freedom. In other words, the orbital ME effect can be finite in systems with only an orbital component. Thus, the orbital ME effect will help detect orbital magnetic orders, and we focus here on a system exhibiting orbital magnetic order, i.e., the loop current order.

Loop currents have been mainly discussed in the pseudogap phase of the high-temperature superconductors [91–97]. Recently, loop-current orders are also discussed as candidates of the time-reversal symmetry breaking charge order in the kagome superconductors AV$_3$Sb$_5$ (A=K, Rb, and Cs) [98,99], the hidden order in the spin-orbit coupled Mott insulator Sr$_2$IrO$_4$ [100–102], the unconventional magnetization at the surface of Sr$_2$RuO$_4$ [103], and the orbital ferromagnetic phase with a loop current in twisted bilayer graphenes [104–107]. Here, we will study the loop-current order in cuprates. Several proposals of loop-current orders exist for this class. We focus here on the $\mathcal{PT}$-symmetric order shown in Fig. 1, where two opposite local currents (red shaded area and blue one) occur. This order is called the LC-Θ_{II} state [91] and belongs to $m'mm$ in the MPG. Thus, only the intrinsic part exists. The model Hamiltonian belonging to $m'mm$ is given by [51,65,96,108]

$$H_{\boldsymbol{k}} = \begin{pmatrix} 0 & its_x + irc_x & its_y + irc_y \\ -its_x - irc_x & 0 & t's_xs_y \\ -its_y - irc_y & t's_xs_y & 0 \end{pmatrix}, \quad (17)$$

where $s_i = \sin(k_i/2a)$ and $c_i = \cos(k_i/2a)$ (a is the lattice constant). This Hamiltonian has no spin degrees of
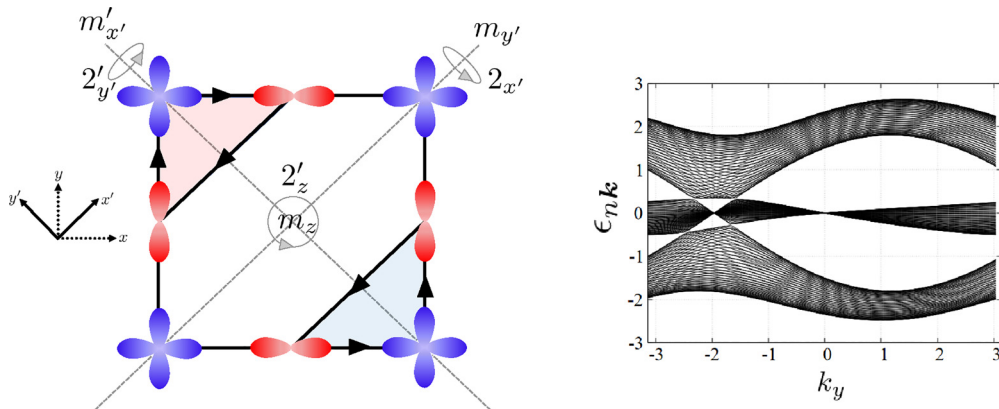
FIG. 1. (Left) Schematic of the loop current on the CuO$_2$ plane. The blue four-leaves and red two-leaves represent the d orbitals on the copper sites and p_x, p_y orbitals on the oxygen sites, respectively. The arrows represent the complex hopping characterizing loop currents. In this case, two z-directional orbital magnetic moments with opposite signs are shown by red and blue shaded areas. The gray letters represent the invariant symmetries in $m'mm$. m_i is the mirror symmetry against the plane vertical to the i axis, and 2_i is the 180° rotational symmetry around the i axis. The symbols with the prime (′), such as $2'_z$, represent the original symmetry multiplied by the time-reversal operation $\mathcal{T}$. This model fulfills $\mathcal{PT}$ symmetry ($\mathcal{PT} = m'_{x'}m_{y'}m_z$). (Right) Band dispersion of our model. This model has four Dirac points at $E = -0.44t$, $-0.27t$, and $0.33t$. We use $\epsilon_{n\boldsymbol{k}}$ in units of t.
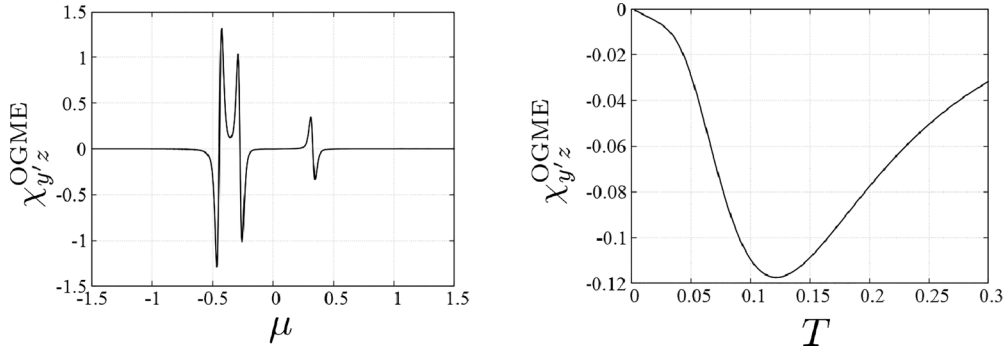
FIG. 2. (Left) The dependence of the OGME tensor on the chemical potential μ at $T/t = 0.01$. (Right) The dependence of the OGME tensor on the temperature at $\mu = -0.8t$. We set $t = 1.0$ and introduce an infinitesimal dissipation $\delta = 0.001i$ for the numerical calculation. We use $\chi_{y'z}^{\text{OGME}}$ in units of $ea/\hbar$, μ, and T in units of t.

freedom because we focus only on the orbital order. The basis consists of the d-orbitals $|d\rangle$ on the copper sites and the p-orbitals $|p_x\rangle$, $|p_y\rangle$ on the oxygen sites. t and t' are hopping constants across these orbitals and r is the order parameter of the loop current. This model has four Dirac points at $E = -0.44t$, $-0.27t$, and $0.33t$, shown in Fig. 1.

Let us discuss the intrinsic OGME tensor for this model. To make the discussion easier, we transform the coordinates from $(k_x, k_y) \rightarrow (k_{x'}, k_{y'})$ as shown in Fig. 1. First, we consider the constraints of symmetry. The group $m'mm$ has the mirror symmetry $m_{y'}$, thus, $\chi_{x'x'}^{\text{iOGME}} = \chi_{x'z}^{\text{iOGME}} = \chi_{y'y'}^{\text{iOGME}} = \chi_{zx'}^{\text{iOGME}} = \chi_{zz}^{\text{iOGME}} = 0$. In addition, this group fulfills the product symmetry of mirror and time-reversal symmetry $m'_{x'}$. Thus, $\chi_{x'y'}^{\text{iOGME}} = \chi_{y'x'}^{\text{iOGME}} = 0$. Therefore, the remaining terms are $\chi_{y'z}^{\text{iOGME}}$ and $\chi_{zy'}^{\text{iOGME}}$.

We calculate $\chi_{y'z}^{\text{iOGME}}$ and show its dependence on the chemical potential μ and the temperature T in Fig. 2. The left figure shows the dependence on the chemical potential at $T/t = 0.01$ where we can see peak structures near the Dirac points. These structures also appear in the orbital ME response [51]. As discussed above, the OGME tensor is determined by the orbital ME tensor [Eq. (14)] and proportional to $\partial\chi_{ij}^{\text{iOGME}}/\partial\mu$ at low temperature. This behavior can be confirmed when comparing this figure with Fig. 2 in Ref. [51]. Next, the right panel in Fig. 2 shows the temperature dependence at $\mu = -0.8t$ where we can confirm the T-linear dependence at low temperature as derived in Eq. (14).

V. CONCLUSIONS

In conclusion, we have discussed the orbital magneto-electric effect induced by a temperature gradient (orbital gravito-ME effect). We have derived its response using a full quantum approach. We have shown that its response is formalized by the second derivative of the current energy-density correlation function. We have calculated the response in periodic systems, and we have shown the appearance of two terms, the extrinsic part and the intrinsic part. We have shown that the intrinsic part needs a correction from the orbital magnetic quadrupole moment. Due to this correction, the intrinsic part has no unphysical divergence and satisfies the

Mott relation. Furthermore, we have demonstrated that the extrinsic part also satisfies the Mott relation. In previous works, the intrinsic part was derived using a semiclassical approach [49,50] without the correction being free of a divergence and satisfying the Mott relation. However, we have demonstrated that this correction is necessary when using the Kubo formula. This fact is an important guideline when calculating the orbital gravito-ME response in strongly correlated systems using Green's function methods.

In addition, we have classified the intrinsic and extrinsic orbital (gravito-) ME responses by the magnetic point groups. We have shown that almost all $\mathcal{PT}$-symmetric groups can be detected by the intrinsic part and have no response in the extrinsic part because the orbital magnetic moment vanishes. We have discussed that the extrinsic part can exist even in systems with time-reversal symmetry because dissipation already breaks this symmetry. The symmetry table of the orbital (gravito-) ME effects is very similar to the table of the nonlinear Hall effects. Thus, the orbital (gravito-) ME effect is also expected in systems where the nonlinear Hall effect occurs.

In experiments, the spin magnetization also contributes to the (gravito-) ME effect. Thus, we need to explore systems with large orbital magnetizations to study the orbital ME effect. Fortunately, phenomena related to orbital magnetic moments, such as the valley Hall effect and the orbital Edelstein effect, have recently been observed in a transition-metal dichalcogenide MoS_2 and twisted bilayer graphene with large orbital magnetic moments around the K points. Thus, the extrinsic OGME effect may also be observable in these systems. On the other hand, the intrinsic part becomes dominant in $\mathcal{PT}$-symmetric orbital magnetic orders, such as an antiferromagnetic loop-current order as discussed in Sec. IV B. There, the intrinsic part is strongly enhanced around the Dirac points. This will give an experimental platform for the detection of the intrinsic orbital (gravito-) ME response.

APPENDIX A: DETAILED CALCULATION OF THE CURRENT ENERGY-DENSITY CORRELATION FUNCTION

The current energy correlation function $\Phi^i_{JH}(\boldsymbol{q}, \omega)$ is given as

$$\Phi^i_{JH}(\boldsymbol{q}, \omega) = -e \sum_{mn,k} \frac{f(\epsilon_{nk+q/2}) - f(\epsilon_{mk-q/2})}{\epsilon_{nk+q/2} - \epsilon_{mk-q/2} - (\omega + i\delta)} \langle u_{mk-q/2}| \, v^i_k \, |u_{nk+q/2}\rangle \frac{\epsilon_{nk+q/2} + \epsilon_{mk-q/2}}{2} \langle u_{nk+q/2}|u_{mk-q/2}\rangle. \quad \text{(A1)}$$

Here, we use the following notations: the eigenenergies are ϵ_{nk}, and the eigenvectors are $|u_{nk}\rangle$, which fulfill $H_k |u_{nk}\rangle = \epsilon_{nk} |u_{nk}\rangle$, where $[H_k = e^{-ik\cdot x}(H_0 - \mu N)e^{ik\cdot x}]$. The velocity operators are defined as $v^i_k = \partial H_k / \partial k_i$, and the Fermi distribution function is $f(\epsilon) = 1/(1 + e^{\beta\epsilon})$. As discussed in the main text, we need to calculate the second-order derivative of the correlation function to obtain the OGME tensor. In the following, we will calculate it for two cases; (A) intraband transitions ($m = n$), and (B) interband transitions ($m \neq n$).

In the case of (A), the correlation function is given as

$$\Phi^{i(A)}_{JH}(\boldsymbol{q}, \omega) = -e \sum_{n,k} \frac{f(\epsilon_{nk+q/2}) - f(\epsilon_{nk-q/2})}{\epsilon_{nk+q/2} - \epsilon_{nk-q/2} - (\omega + i\delta)} \langle u_{nk-q/2}| \, v^i_k \, |u_{nk+q/2}\rangle \frac{\epsilon_{nk+q/2} + \epsilon_{nk-q/2}}{2} \langle u_{nk+q/2}|u_{nk-q/2}\rangle. \quad \text{(A2)}$$

We expand each coefficient up to the second order of $\boldsymbol{q}$,

$$\frac{f(\epsilon_{nk+q/2}) - f(\epsilon_{nk-q/2})}{\epsilon_{nk+q/2} - \epsilon_{nk-q/2} - (\omega + i\delta)} \simeq \frac{-f'_n(\partial_a \epsilon_n) q_a}{\omega + i\delta} - \frac{f'_n(\partial_a \epsilon_n)(\partial_b \epsilon_n) q_a q_b}{(\omega + i\delta)^2}, \quad \text{(A3a)}$$

$$\frac{\epsilon_{nk+q/2} + \epsilon_{nk-q/2}}{2} \simeq \epsilon_{nk} + 0, \quad \text{(A3b)}$$

$$\langle u_{nk+q/2}|u_{nk-q/2}\rangle \simeq 1 - q_a \langle u_{nk}|\partial_a u_{nk}\rangle, \quad \text{(A3c)}$$

$$\langle u_{nk-q/2}| \, v^i_k \, |u_{nk+q/2}\rangle \simeq \partial_i \epsilon_{nk} + \frac{q_a}{2}(\langle u_{nk}| \, v^i_k \, |\partial_a u_{nk}\rangle - \langle \partial_a u_{nk}| \, v^i_k \, |u_{nk}\rangle). \quad \text{(A3d)}$$

Here, we define $f'_n = \partial f(\epsilon_{nk})/\partial \epsilon_{nk}$. Then, the second derivative of $\Phi^{i(A)}_{JH}(\boldsymbol{q}, \omega)$ for intraband transitions is

$$\Phi^{i,ab(A)}_{JH}(\omega) q_a q_b = -e \sum_{n,k} \epsilon_{nk} \left[\frac{-f'_n(\partial_a \epsilon_{nk})}{\omega + i\delta} \left(-(\partial_i \epsilon_{nk}) \langle u_{nk}|\partial_b u_{nk}\rangle + \frac{1}{2}(\langle u_{nk}| \, v^i_k \, |\partial_b u_{nk}\rangle - \langle \partial_b u_{nk}| \, v^i_k \, |u_{nk}\rangle) \right) \right.$$
$$\left. - \frac{f'_n}{(\omega + i\delta)^2}(\partial_a \epsilon_{nk})(\partial_b \epsilon_{nk})(\partial_i \epsilon_{nk}) \right] q_a q_b. \quad \text{(A4)}$$

The term proportional to $1/(\omega + i\delta)^1$ can be transformed as

$$-(\partial_i \epsilon_{nk}) \langle u_{nk}|\partial_b u_{nk}\rangle + \tfrac{1}{2}(\langle u_{nk}| \, v^i_k \, |\partial_b u_{nk}\rangle - \langle \partial_b u_{nk}| \, v^i_k \, |u_{nk}\rangle) = \tfrac{1}{2}(\langle u_{nk}| \, v^i_k Q_n \, |\partial_b u_{nk}\rangle - \langle \partial_b u_{nk}| \, Q_n v^i_k \, |u_{nk}\rangle)$$
$$= \tfrac{1}{2}(\langle \partial_i u_{nk}| \, \epsilon_n - H_k \, |\partial_b u_{nk}\rangle - \text{c.c.}) \equiv m^{ib}_n - (\text{c.c.}). \quad \text{(A5)}$$

Here, we define $Q_n = 1 - |u_{nk}\rangle \langle u_{nk}|$. Using this identity, we can write the correlation function $\Phi^{i,ab(A)}_{JH}(\omega)$ as

$$\Phi^{i,ab(A)}_{JH}(\omega) q_a q_b = -e \sum_{n,k} \epsilon_{nk} \left[\frac{-f'_n}{\omega + i\delta}(\partial_a \epsilon_{nk})(m^{ib}_n - m^{bi}_n) - \frac{f'_n}{(\omega + i\delta)^2}(\partial_a \epsilon_{nk})(\partial_b \epsilon_{nk})(\partial_i \epsilon_{nk}) \right] q_a q_b. \quad \text{(A6)}$$

Finally, we use Eq. (3b) and obtain the contribution from the current energy-density correlation function to the OGME tensor as

$$2i\beta^{JH(A)}_{li} = \frac{2}{3}\varepsilon_{ijk}\Phi^{k,lj(A)}_{JH}(0) = -\frac{e}{\delta} \sum_{n,k} \epsilon_{nk} f'_n \left\{ (\partial_l \epsilon_{nk}) m^i_n - \frac{1}{3}\delta_{li}(\partial_j \epsilon_{nk}) m^j_n \right\}. \quad \text{(A7)}$$

Here, $\boldsymbol{m}_n = \text{Im}[\langle \nabla u_{nk}| \times (\epsilon_{nk} - H_k) |\nabla u_{nk}\rangle]/2$ is the orbital magnetic moment. This tensor has a Drude-like singularity and originates from the Fermi surface. It is the extrinsic response and is called the Edelstein effect.

Next, we consider the case of interband transitions (B). In this case, the denominator has no singularity. Thus, we can take the limits $\omega, \delta \to 0$. The correlation function is given as

$$\Phi^{i(B)}_{JH}(\boldsymbol{q}, \omega) = -e \sum_{m \neq n,k} \frac{f(\epsilon_{nk+q/2}) - f(\epsilon_{mk-q/2})}{\epsilon_{nk+q/2} - \epsilon_{mk-q/2}} \langle u_{mk-q/2}| \, v^i_k \, |u_{nk+q/2}\rangle \frac{\epsilon_{nk+q/2} + \epsilon_{mk-q/2}}{2} \langle u_{nk+q/2}|u_{mk-q/2}\rangle. \quad \text{(A8)}$$

Expanding each coefficients by $\boldsymbol{q}$ up to the second order,

$$\langle u_{nk+q/2}|u_{mk-q/2}\rangle \simeq -q_a \langle u_{nk}|\partial_a u_{mk}\rangle - \frac{q_a q_b}{2} \langle \partial_a u_{nk}|\partial_b u_{mk}\rangle, \tag{A9a}$$

$$\frac{\epsilon_{nk+q/2} + \epsilon_{mk-q/2}}{2} \simeq \frac{\tilde{\epsilon}_{nmk}}{2} + \frac{q_a}{4}\partial_a \epsilon_{nmk}, \tag{A9b}$$

$$\langle u_{mk-q/2}| v_k^i |u_{nk+q/2}\rangle \simeq i\epsilon_{mnk}\mathcal{A}_{mn}^i - \frac{q_a}{2}(\langle \partial_a u_{mk}| v_k^i |u_{nk}\rangle - \langle u_{mk}| v_k^i |\partial_a u_{nk}\rangle)$$

$$= -\epsilon_{mnk} \langle u_{mk}|\partial_i u_{nk}\rangle - \frac{q_a}{2}\left(-\partial_i\tilde{\epsilon}_{nmk} \langle u_{mk}|\partial_a u_{nk}\rangle - \sum_{l(\neq n)} \langle \partial_a u_{mk}|u_{lk}\rangle \epsilon_{lnk} \langle u_{lk}|\partial_i u_{nk}\rangle \right.$$

$$\left. + \sum_{l(\neq m)} \epsilon_{mlk} \langle u_{mk}|\partial_i u_{lk}\rangle \langle u_{lk}|\partial_a u_{nk}\rangle \right), \tag{A9c}$$

$$\frac{f(\epsilon_{nk+q/2}) - f(\epsilon_{mk-q/2})}{\epsilon_{nk+q/2} - \epsilon_{mk-q/2}} \simeq \frac{f_{nm}}{\epsilon_{nmk}} + \frac{q_a}{2\epsilon_{nmk}}\left(\partial_a \tilde{f}_{nm} - \frac{(\partial_a\tilde{\epsilon}_{nmk})f_{nm}}{\epsilon_{nmk}} \right). \tag{A9d}$$

Here, we define $\epsilon_{nmk} = \epsilon_{nk} - \epsilon_{mk}, \tilde{\epsilon}_{nmk} = \epsilon_{nk} + \epsilon_{mk}, f_{nm} = f(\epsilon_{nk}) - f(\epsilon_{mk})$, and $\tilde{f}_{nm} = f(\epsilon_{nk}) + f(\epsilon_{mk})$. $\mathcal{A}_{mn}^i = i \langle u_{mk}|\partial_i u_{nk}\rangle$ is the Berry connection. To simplify the calculation, we split the second-order derivative into two cases with respect to Eq. (A9b): (i) the contribution from the first term and (ii) the contribution from the second term. In the case of (i), the second derivative of the correlation function is

$$\Phi_{JH}^{i,ab(\mathrm{B-i})}q_a q_b = -e \sum_{m\neq nk} \frac{\tilde{\epsilon}_{nmk}}{2}\left\{ -\frac{f_{nm}}{2} \langle u_{mk}|\partial_i u_{nk}\rangle \langle \partial_a u_{nk}|\partial_b u_{mk}\rangle + \frac{f_{nm}}{2\epsilon_{nmk}} \langle u_{nk}|\partial_a u_{mk}\rangle \right.$$

$$\times \left(-\partial_i\tilde{\epsilon}_{nmk} \langle u_{mk}|\partial_b u_{nk}\rangle - \sum_{l(\neq n)} \langle \partial_b u_{mk}|u_{lk}\rangle \epsilon_{lnk} \langle u_{lk}|\partial_i u_{nk}\rangle + \sum_{l(\neq m)} \epsilon_{mlk} \langle u_{mk}|\partial_i u_{lk}\rangle \langle u_{lk}|\partial_b u_{nk}\rangle \right)$$

$$\left. -\frac{1}{2} \langle u_{nk}|\partial_a u_{mk}\rangle \langle u_{mk}|\partial_i u_{nk}\rangle \left(\partial_b\tilde{f}_{nm} - \frac{(\partial_b\tilde{\epsilon}_{nmk})f_{nm}}{\epsilon_{nmk}} \right) \right\}q_a q_b$$

$$= -e \sum_{m\neq nk} \frac{\tilde{\epsilon}_{nmk}}{2}\left\{ -f_n\mathrm{Re}[\langle u_{mk}|\partial_i u_{nk}\rangle \langle \partial_a u_{nk}|\partial_b u_{mk}\rangle] + \frac{f_n}{\epsilon_{nmk}}\left(-\partial_i\tilde{\epsilon}_{nmk}\mathrm{Re}[\langle u_{nk}|\partial_a u_{mk}\rangle \langle u_{mk}|\partial_b u_{nk}\rangle] \right. \right.$$

$$\left. -\sum_{l(\neq n)} \epsilon_{lnk}\mathrm{Re}[\langle u_{nk}|\partial_a u_{mk}\rangle \langle \partial_b u_{mk}|u_{lk}\rangle \langle u_{lk}|\partial_i u_{nk}\rangle] + \sum_{l(\neq m)} \epsilon_{mlk}\mathrm{Re}[\langle u_{nk}|\partial_a u_{mk}\rangle \langle u_{mk}|\partial_i u_{lk}\rangle \langle u_{lk}|\partial_b u_{nk}\rangle] \right)$$

$$\left. -\mathrm{Re}[\langle u_{nk}|\partial_a u_{mk}\rangle \langle u_{mk}|\partial_i u_{nk}\rangle]\left(\partial_b f_n - \frac{(\partial_b\tilde{\epsilon}_{nmk})f_n}{\epsilon_{nmk}} \right) \right\}q_a q_b. \tag{A10}$$

We split this further into two parts regarding the denominator; (a) $(\epsilon_{nmk})^0$ and (b) $(\epsilon_{nmk})^1$ in the denominator. In the case of (a), collecting the terms whose denominator is $(\epsilon_{nmk})^0$, we obtain

$$\Phi_{JH}^{i,ab(\mathrm{B-i-a})}q_a q_b = -e \sum_{m\neq n,k}\left[\frac{\tilde{\epsilon}_{nmk}}{2}\left\{ -f_n\mathrm{Re}[\langle u_{mk}|\partial_i u_{nk}\rangle \langle \partial_a u_{nk}|\partial_b u_{mk}\rangle] - (\partial_b f_n)\mathrm{Re}[\langle u_{nk}|\partial_a u_{mk}\rangle \langle u_{mk}|\partial_i u_{nk}\rangle] \right. \right.$$

$$\left. + f_n \sum_{l(\neq n)} \mathrm{Re}[\langle u_{nk}|\partial_a u_{mk}\rangle \langle \partial_b u_{mk}|u_{lk}\rangle \langle u_{lk}|\partial_i u_{nk}\rangle] - f_n\mathrm{Re}[\langle u_{nk}|\partial_a u_{mk}\rangle \langle u_{mk}|\partial_i u_{nk}\rangle \langle u_{nk}|\partial_b u_{nk}\rangle] \right\}$$

$$+ \frac{f_n}{2}(\partial_i\tilde{\epsilon}_{nmk})\mathrm{Re}[\langle u_{nk}|\partial_a u_{mk}\rangle \langle u_{mk}|\partial_b u_{nk}\rangle] - \frac{f_n}{2}(\partial_b\tilde{\epsilon}_{nmk})\mathrm{Re}[\langle u_{nk}|\partial_a u_{mk}\rangle \langle u_{mk}|\partial_i u_{nk}\rangle]$$

$$+ \frac{f_n}{2}\sum_{l(\neq n)} \epsilon_{lmk}\mathrm{Re}[\langle u_{nk}|\partial_a u_{mk}\rangle \langle \partial_b u_{mk}|u_{lk}\rangle \langle u_{lk}|\partial_i u_{nk}\rangle]$$

$$+ \frac{f_n}{2}\sum_{l(\neq n)} \epsilon_{lmk}\mathrm{Re}[\langle u_{nk}|\partial_a u_{mk}\rangle \langle u_{mk}|\partial_i u_{lk}\rangle \langle u_{lk}|\partial_b u_{nk}\rangle]\right]q_a q_b$$

$$
\begin{aligned}
= -e \sum_{m\neq n,\mathbf{k}} \frac{f_n}{2} \Bigg\{ &-\tilde{\epsilon}_{nmk}\mathrm{Re}[\langle u_{mk}|\partial_i u_{nk}\rangle\langle\partial_a u_{nk}|\partial_b u_{mk}\rangle] \\
&+ \tilde{\epsilon}_{nmk}\partial_b\mathrm{Re}[\langle u_{nk}|\partial_a u_{mk}\rangle\langle u_{mk}|\partial_i u_{nk}\rangle] + \sum_{l(\neq n)}\tilde{\epsilon}_{nlk}\mathrm{Re}[\langle u_{nk}|\partial_a u_{mk}\rangle\langle\partial_b u_{mk}|u_{lk}\rangle\langle u_{lk}|\partial_i u_{nk}\rangle] \\
&- \tilde{\epsilon}_{nmk}\mathrm{Re}[\langle u_{nk}|\partial_a u_{mk}\rangle\langle u_{mk}|\partial_i u_{nk}\rangle\langle u_{nk}|\partial_b u_{nk}\rangle] + (\partial_i\tilde{\epsilon}_{nmk})\mathrm{Re}[\langle u_{nk}|\partial_a u_{mk}\rangle\langle u_{mk}|\partial_b u_{nk}\rangle] \\
&+ \sum_{l(\neq n)}\epsilon_{lmk}\mathrm{Re}[\langle u_{nk}|\partial_a u_{mk}\rangle\langle u_{mk}|\partial_i u_{lk}\rangle\langle u_{lk}|\partial_b u_{nk}\rangle] \Bigg\} q_a q_b.
\end{aligned}
\tag{A11}
$$

The third term in this equation can be transformed as

$$
\begin{aligned}
\sum_{l(\neq n),m(\neq n)}\tilde{\epsilon}_{nlk}\mathrm{Re}[\langle u_{nk}|\partial_a u_{mk}\rangle\langle\partial_b u_{mk}|u_{lk}\rangle\langle u_{lk}|\partial_i u_{nk}\rangle] = \sum_{l(\neq n)}\tilde{\epsilon}_{nlk}\{&\mathrm{Re}[\langle\partial_a u_{nk}|\partial_b u_{lk}\rangle\langle u_{lk}|\partial_i u_{nk}\rangle] \\
&- \mathrm{Re}[\langle\partial_a u_{nk}|u_{nk}\rangle\langle u_{nk}|\partial_b u_{lk}\rangle\langle u_{lk}|\partial_i u_{nk}\rangle]\}.
\end{aligned}
\tag{A12}
$$

Therefore, this term cancels out the first and fourth terms. Finally, we get

$$
\Phi_{JH}^{i,ab(\mathrm{B-i-a})}q_a q_b = -e\sum_{n\neq m,\mathbf{k}}\left\{ \frac{\tilde{\epsilon}_{nmk}f_n}{2}\left(-\partial_b\mathrm{Re}\big[\mathcal{A}_{nm}^a\mathcal{A}_{mn}^i\big]\right) - f_n\sum_{l(\neq n)}\mathrm{Re}\big[\mathcal{A}_{nm}^a V_{ml,n}^i \mathcal{A}_{ln}^b\big]\right\}q_a q_b.
\tag{A13}
$$

Here, we define $V_{lm,n}^i = \frac{1}{2}(v_{lm}^i + v_n^{0i}\delta_{lm})$. In the case of (b), collecting the terms whose denominator is $(\epsilon_{nmk})^1$,

$$
\begin{aligned}
\Phi_{JH}^{i,ab(\mathrm{B-i-b})}q_a q_b = -e\sum_{m\neq n,\mathbf{k}}\frac{\epsilon_{nk}f_n}{\epsilon_{nmk}}\Bigg\{ &-(\partial_i\tilde{\epsilon}_{nmk})\mathrm{Re}[\langle u_{nk}|\partial_a u_{mk}\rangle]\langle u_{mk}|\partial_b u_{nk}\rangle + (\partial_b\tilde{\epsilon}_{nmk})\mathrm{Re}[\langle u_{nk}|\partial_a u_{mk}\rangle]\langle u_{mk}|\partial_i u_{nk}\rangle \\
&- \sum_{l(\neq n)}\epsilon_{lmk}\mathrm{Re}[\langle u_{nk}|\partial_a u_{mk}\rangle\langle\partial_b u_{mk}|u_{lk}\rangle\langle u_{lk}|\partial_i u_{nk}\rangle] + \sum_{l(\neq n)}\epsilon_{mlk}\mathrm{Re}[\langle u_{nk}|\partial_a u_{mk}\rangle\langle u_{mk}|\partial_i u_{lk}\rangle\langle u_{lk}|\partial_b u_{nk}\rangle]\Bigg\}q_a q_b \\
= -e\sum_{m\neq n,\mathbf{k}}\frac{2\epsilon_{nk}f_n}{\epsilon_{nmk}}\sum_{l(\neq n)}&\left\{-\mathrm{Re}[\mathcal{A}_{nm}^a V_{ml,n}^b \mathcal{A}_{ln}^i] + \mathrm{Re}[\mathcal{A}_{nm}^a V_{ml,n}^i \mathcal{A}_{ln}^b]\right\}q_a q_b.
\end{aligned}
\tag{A14}
$$

Next, calculating the case of (ii), we get

$$
\Phi_{JH}^{i,ab(\mathrm{B-ii})}q_a q_b = -e\sum_{m\neq n,\mathbf{k}}\frac{f_n}{2}(\partial_b\epsilon_{nmk})\mathrm{Re}[\mathcal{A}_{nm}^a\mathcal{A}_{mn}^i]q_a q_b.
\tag{A15}
$$

Collecting all terms, we obtain

$$
\begin{aligned}
\Phi_{JH}^{i,ab(\mathrm{B})}q_a q_b = -e\sum_{n,\mathbf{k}}\Bigg[\epsilon_{nk}f_n\sum_{m(\neq n)}&\left\{-\partial_b\mathrm{Re}\big[\mathcal{A}_{nm}^a\mathcal{A}_{mn}^i\big] + \frac{2}{\epsilon_{nmk}}\sum_{l(\neq n)}\left(-\mathrm{Re}\big[\mathcal{A}_{nm}^a V_{ml,n}^b \mathcal{A}_{ln}^i\big] + \mathrm{Re}\big[\mathcal{A}_{nm}^a V_{ml,n}^i \mathcal{A}_{ln}^b\big]\right)\right\} \\
&+ f_n\left\{-\sum_{m(\neq n)}\sum_{l(\neq n)}\mathrm{Re}\big[\mathcal{A}_{nm}^a V_{ml,n}^i \mathcal{A}_{ln}^b\big] + \frac{1}{4}\frac{\partial^3\epsilon_{nk}}{\partial k_i\partial k_a\partial k_b} - \frac{1}{4}\partial_b v_n^{ia}\right\}\Bigg]q_a q_b.
\end{aligned}
\tag{A16}
$$

Here, we define $v_n^{ia} = \langle u_{nk}|\partial^2 H_k/\partial k_i\partial k_a|u_{nk}\rangle$. Finally, we use Eq. (3b) and obtain the contribution from the current energy-density correlation function to the OGME tensor as

$$
\begin{aligned}
2i\beta_{li}^{JH(\mathrm{B})} = \frac{2}{3}\varepsilon_{ijk}\Phi_{JH}^{k,lj(\mathrm{B})} = -e\sum_{nk}\Bigg[&\epsilon_{nk}f_n\left\{-\frac{1}{3}\varepsilon_{ijk}\partial_j g_n^{lk} - \sum_{m(\neq n)}\frac{2}{\epsilon_{nmk}}\mathrm{Re}\left[\mathcal{A}_{nm}^l M_{mn}^i - \frac{1}{3}\delta_{li}\mathcal{A}_{nm}^j M_{mn}^j\right]\right\} \\
&+ f_n\left\{\frac{2}{3}\sum_{m(\neq n)}\mathrm{Re}\big[\mathcal{A}_{nm}^l M_{mn}^i\big] - \frac{1}{12}\varepsilon_{ijk}\partial_j v_n^{kl}\right\}\Bigg].
\end{aligned}
\tag{A17}
$$

Here, we use the quantum metric $g_n^{lk} = \sum_{m(\neq n)}\mathrm{Re}[\mathcal{A}_{nm}^l\mathcal{A}_{mn}^k]$ and $\boldsymbol{M}_{mn} = \sum_{l(\neq n)}\boldsymbol{V}_{ml,n}\times\mathcal{A}_{ln}$. This equation does not depend on the dissipation in the clean limit. Thus, it can be regarded as the intrinsic part.

APPENDIX B: DERIVATION OF THE MOTT RELATION [EQS. ([14](#)) AND ([16](#))]

The intrinsic OGME tensor and the intrinsic OME tensor at the chemical potential μ and at the temperature T are defined as

$$\chi_{ij}^{\text{iOGME}}(\mu, T) = e \int_{\text{BZ}} \frac{d^3k}{(2\pi)^3} \sum_n s(\epsilon_{n\boldsymbol{k}}) W_{ij}^n, \tag{B1}$$

$$\chi_{ij}^{\text{iOME}}(\mu, T) = -e^2 \int_{\text{BZ}} \frac{d^3k}{(2\pi)^3} \sum_n f(\epsilon_{n\boldsymbol{k}}) W_{ij}^n. \tag{B2}$$

Here, $f(\epsilon) = 1/(1 + e^{\beta\epsilon})$ is the distribution function at the inverse temperature $\beta = 1/T$ and $s(\epsilon) = \epsilon f(\epsilon)/T + \ln(1 + e^{-\beta\epsilon})$ is the entropy density. W_{ij}^n represents the wave-function part in Eq. ([13](#)). The OGME tensor can be rewritten as

$$\chi_{ij}^{\text{iOGME}}(\mu, T) = e \int_{\text{BZ}} \frac{d^3k}{(2\pi)^3} \sum_n s(\epsilon_{n\boldsymbol{k}}) W_{ij}^n = e \int_{\text{BZ}} \frac{d^3k}{(2\pi)^3} \int d\epsilon \sum_n s(\epsilon) W_{ij}^n \delta(\epsilon - \epsilon_{n\boldsymbol{k}})$$

$$= e \int_{\text{BZ}} \frac{d^3k}{(2\pi)^3} \int d\epsilon \sum_n s(\epsilon) W_{ij}^n \frac{d\Theta(\epsilon - \epsilon_{n\boldsymbol{k}})}{d\epsilon} = \frac{-1}{e} \int d\epsilon\, s(\epsilon) \frac{\partial \chi_{ij}^{\text{iOME}}(\epsilon + \mu, 0)}{\partial \epsilon}$$

$$= \frac{1}{eT} \int d\epsilon (\epsilon - \mu) \frac{\partial f(\epsilon - \mu)}{\partial \epsilon} \chi_{ij}^{\text{iOME}}(\epsilon, 0). \tag{B3}$$

In the final step, we use partial integration and the identity $\partial s(\epsilon)/\partial\epsilon = \beta\epsilon[\partial f(\epsilon)/\partial\epsilon]$. Here, $\delta(x)$ is the δ function, and $\Theta(x)$ is the step function. This formula is called the Mott relation.

The Mott formula is also established for the extrinsic part. The extrinsic OGME tensor and the extrinsic OME tensor at the chemical potential μ and at the temperature T are given by

$$\chi_{ij}^{\text{eOGME}}(\mu, T) = \frac{e}{\delta T} \int_{\text{BZ}} \frac{d^3k}{(2\pi)^3} \sum_n \epsilon_{n\boldsymbol{k}} \frac{\partial f(\epsilon_{n\boldsymbol{k}})}{\partial \epsilon_{n\boldsymbol{k}}} \tilde{W}_{ij}^n, \tag{B4}$$

$$\chi_{ij}^{\text{eOME}}(\mu, T) = \frac{-e^2}{\delta} \int_{\text{BZ}} \frac{d^3k}{(2\pi)^3} \sum_n \frac{\partial f(\epsilon_{n\boldsymbol{k}})}{\partial \epsilon_{n\boldsymbol{k}}} \tilde{W}_{ij}^n. \tag{B5}$$

Here, $\tilde{W}_{ij}^n$ represents the wave-function part in Eq. ([15](#)). The extrinsic OGME tensor can be rewritten as

$$\chi_{ij}^{\text{eOGME}}(\mu, T) = \frac{e}{\delta T} \int_{\text{BZ}} \frac{d^3k}{(2\pi)^3} \sum_n \epsilon_{n\boldsymbol{k}} \frac{\partial f(\epsilon_{n\boldsymbol{k}})}{\partial \epsilon_{n\boldsymbol{k}}} \tilde{W}_{ij}^n = \frac{e}{\delta T} \int_{\text{BZ}} \frac{d^3k}{(2\pi)^3} \int d\epsilon \sum_n \epsilon \frac{\partial f(\epsilon)}{\partial \epsilon} \tilde{W}_{ij}^n \frac{d\Theta(\epsilon - \epsilon_{n\boldsymbol{k}})}{d\epsilon}$$

$$= \frac{1}{eT} \int d\epsilon\, \epsilon \frac{\partial f(\epsilon)}{\partial \epsilon} \chi_{ij}^{\text{eOME}}(\epsilon + \mu, 0) = \frac{1}{eT} \int d\epsilon (\epsilon - \mu) \frac{\partial f(\epsilon - \mu)}{\partial \epsilon} \chi_{ij}^{\text{eOME}}(\epsilon, 0). \tag{B6}$$

Therefore, the extrinsic part also satisfies the Mott relation.

[1] T. Thonhauser, D. Ceresoli, D. Vanderbilt, and R. Resta, Orbital Magnetization in Periodic Insulators, Phys. Rev. Lett. **95**, 137205 (2005).

[2] D. Ceresoli, T. Thonhauser, D. Vanderbilt, and R. Resta, Orbital magnetization in crystalline solids: Multi-band insulators, chern insulators, and metals, Phys. Rev. B **74**, 024408 (2006).

[3] D. Xiao, J. Shi, and Q. Niu, Berry Phase Correction to Electron Density of States in Solids, Phys. Rev. Lett. **95**, 137204 (2005).

[4] J. Shi, G. Vignale, D. Xiao, and Q. Niu, Quantum Theory of Orbital Magnetization and Its Generalization to Interacting Systems, Phys. Rev. Lett. **99**, 197202 (2007).

[5] D. Vanderbilt, *Berry Phases in Electronic Structure Theory: Electric Polarization, Orbital Magnetization and Topological Insulators* (Cambridge University Press, Cambridge, UK, 2018).

[6] D. Xiao, W. Yao, and Q. Niu, Valley-Contrasting Physics in Graphene: Magnetic Moment and Topological Transport, Phys. Rev. Lett. **99**, 236809 (2007).

[7] K. F. Mak, K. L. McGill, J. Park, and P. L. McEuen, The valley hall effect in MoS$_2$ transistors, Science **344**, 1489 (2014).

[8] D. Go, D. Jo, H.-W. Lee, M. Kläui, and Y. Mokrousov, Orbitronics: Orbital currents in solids, Europhys. Lett. **135**, 37001 (2021).

[9] D. Go and H.-W. Lee, Orbital torque: Torque generation by orbital current injection, Phys. Rev. Res. **2**, 013177 (2020).

[10] D. Go, F. Freimuth, J.-P. Hanke, F. Xue, O. Gomonay, K.-J. Lee, S. Blügel, P. M. Haney, H.-W. Lee, and Y. Mokrousov, Theory of current-induced angular momentum transfer dynamics in spin-orbit coupled systems, Phys. Rev. Res. **2**, 033401 (2020).

[11] S. Ding, A. Ross, D. Go, L. Baldrati, Z. Ren, F. Freimuth, S. Becker, F. Kammerbauer, J. Yang, G. Jakob, Y. Mokrousov,

and M. Kläui, Harnessing Orbital-to-Spin Conversion of Interfacial Orbital Currents for Efficient Spin-Orbit Torques, Phys. Rev. Lett. **125**, 177201 (2020).

[12] S. Lee, M.-G. Kang, D. Go, D. Kim, J.-H. Kang, T. Lee, G.-H. Lee, J. Kang, N. J. Lee, Y. Mokrousov *et al.*, Efficient conversion of orbital hall current to spin current for spin-orbit torque switching, Commun. Phys. **4**, 234 (2021).

[13] J. Kim, D. Go, H. Tsai, D. Jo, K. Kondou, H.-W. Lee, and YoshiChika Otani, Nontrivial torque generation by orbital angular momentum injection in ferromagnetic-metal/Cu/Al_2O_3 trilayers, Phys. Rev. B **103**, L020407 (2021).

[14] S. Ding, Z. Liang, D. Go, C. Yun, M. Xue, Z. Liu, S. Becker, W. Yang, H. Du, C. Wang, Y. Yang, G. Jakob, M. Kläui, Y. Mokrousov, and J. Yang, Observation of the Orbital Rashba-Edelstein Magnetoresistance, Phys. Rev. Lett. **128**, 067201 (2022).

[15] D. Lee, D. Go, H.-J. Park, W. Jeong, H.-W. Ko, D. Yun, D. Jo, S. Lee, G. Go, J. H. Oh *et al.*, Orbital torque in magnetic bilayers, Nat. Commun. **12**, 6710 (2021).

[16] X.-G. Ye, P.-F. Zhu, W.-Z. Xu, N. Shang, K. Liu, and Z.-M. Liao, Orbit-transfer torque driven field-free switching of perpendicular magnetization, Chin. Phys. Lett. **39**, 037303 (2022).

[17] I. E. Dzyaloshinskii, On the magneto-electrical effects in antiferromagnets, Sov. Phys. JETP **10**, 628 (1960).

[18] D. N. Astrov, The magnetoelectric effect in antiferromagnetics, Sov. Phys. JETP **11**, 708 (1960).

[19] V. J. Folen, G. T. Rado, and E. W. Stalder, Anisotropy of the Magnetoelectric Effect in Cr_2O_3, Phys. Rev. Lett. **6**, 607 (1961).

[20] M. Fiebig, Revival of the magnetoelectric effect, J. Phys. D: Appl. Phys. **38**, R123 (2005).

[21] Y. Wang, J. Hu, Y. Lin, and C.-W. Nan, Multiferroic magnetoelectric composite nanostructures, NPG Asia Mater. **2**, 61 (2010).

[22] Y. Tokura, S. Seki, and N. Nagaosa, Multiferroics of spin origin, Rep. Prog. Phys. **77**, 076501 (2014).

[23] S. Dong, J.-M. Liu, S.-W. Cheong, and Z. Ren, Multiferroic materials and magnetoelectric physics: Symmetry, entanglement, excitation, and topology, Adv. Phys. **64**, 519 (2015).

[24] M. Fiebig, T. Lottermoser, D. Meier, and M. Trassin, The evolution of multiferroics, Nat. Rev. Mater. **1**, 16046 (2016).

[25] V. M. Edelstein, Spin polarization of conduction electrons induced by electric current in two-dimensional asymmetric electron systems, Solid State Commun. **73**, 233 (1990).

[26] X.-L. Qi, T. L. Hughes, and S.-C. Zhang, Topological field theory of time-reversal invariant insulators, Phys. Rev. B **78**, 195424 (2008).

[27] A. M. Essin, J. E. Moore, and D. Vanderbilt, Magnetoelectric Polarizability and Axion Electrodynamics in Crystalline Insulators, Phys. Rev. Lett. **102**, 146805 (2009).

[28] A. Malashevich, I. Souza, S. Coh, and D. Vanderbilt, Theory of orbital magnetoelectric response, New J. Phys. **12**, 053032 (2010).

[29] A. Malashevich and I. Souza, Band theory of spatial dispersion in magnetoelectrics, Phys. Rev. B **82**, 245118 (2010).

[30] Y. Gao, S. A. Yang, and Q. Niu, Field Induced Positional Shift of Bloch Electrons and Its Dynamical Implications, Phys. Rev. Lett. **112**, 166601 (2014).

[31] A. Sekine and K. Nomura, Axion electrodynamics in topological materials, J. Appl. Phys. **129**, 141101 (2021).

[32] L. Wu, M. Salehi, N. Koirala, J. Moon, S. Oh, and N. P. Armitage, Quantized faraday and Kerr rotation and axion electrodynamics of a 3D topological insulator, Science **354**, 1124 (2016).

[33] K. N. Okada, Y. Takahashi, M. Mogi, R. Yoshimi, A. Tsukazaki, K. S. Takahashi, N. Ogawa, M. Kawasaki, and Y. Tokura, Terahertz spectroscopy on faraday and Kerr rotations in a quantum anomalous hall state, Nat. Commun. **7**, 12245 (2016).

[34] C. Liu, Y. Wang, H. Li, Y. Wu, Y. Li, J. Li, K. He, Y. Xu, J. Zhang, and Y. Wang, Robust axion insulator and chern insulator phases in a two-dimensional antiferromagnetic topological insulator, Nature Mater. **19**, 522 (2020).

[35] A. Gao, Y.-F. Liu, C. Hu, J.-X. Qiu, C. Tzschaschel, B. Ghosh, S.-C. Ho, D. Bérubé, R. Chen, H. Sun *et al.*, Layer hall effect in a 2D topological axion antiferromagnet, Nature (London) **595**, 521 (2021).

[36] L. S. Levitov, Y. V. Nazarov, and G. M. Eliashberg, Magnetoelectric effects in conductors with mirror isomer symmetry, Sov. Phys. JETP **61**, 133 (1985).

[37] T. Yoda, T. Yokoyama, and S. Murakami, Current-induced orbital and spin magnetizations in crystals with helical structure, Sci. Rep. **5**, 12024 (2015).

[38] S. Zhong, J. E. Moore, and I. Souza, Gyrotropic Magnetic Effect and the Magnetic Moment on the Fermi Surface, Phys. Rev. Lett. **116**, 077201 (2016).

[39] D. Hara, M. S. Bahramy, and S. Murakami, Current-induced orbital magnetization in systems without inversion symmetry, Phys. Rev. B **102**, 184404 (2020).

[40] S. Bhowal and S. Satpathy, Orbital gyrotropic magnetoelectric effect and its strain engineering in monolayer NbX_2, Phys. Rev. B **102**, 201403(R) (2020).

[41] J. Rou, C. Şahin, J. Ma, and D. A. Pesin, Kinetic orbital moments and nonlocal transport in disordered metals with nontrivial band geometry, Phys. Rev. B **96**, 035120 (2017).

[42] C. Niu, J.-P. Hanke, P. M. Buhl, H. Zhang, L. Plucinski, D. Wortmann, S. Blügel, G. Bihlmayer, and Y. Mokrousov, Mixed topological semimetals driven by orbital complexity in two-dimensional ferromagnets, Nat. Commun. **10**, 3179 (2019).

[43] J. Lee, Z. Wang, H. Xie, K. F. Mak, and J. Shan, Valley magnetoelectricity in single-layer MoS_2, Nature Mater. **16**, 887 (2017).

[44] J. Son, K.-H. Kim, Y. H. Ahn, H.-W. Lee, and J. Lee, Strain Engineering of the Berry Curvature Dipole and Valley Magnetization in Monolayer MoS_2, Phys. Rev. Lett. **123**, 036806 (2019).

[45] A. L. Sharpe, E. J. Fox, A. W. Barnard, J. Finney, K. Watanabe, T. Taniguchi, M. A. Kastner, and D. Goldhaber-Gordon, Emergent ferromagnetism near three-quarters filling in twisted bilayer graphene, Science **365**, 605 (2019).

[46] W.-Y. He, D. Goldhaber-Gordon, and K. T. Law, Giant orbital magnetoelectric effect and current-induced magnetization switching in twisted bilayer graphene, Nat. Commun. **11**, 1 (2020).

[47] W.-Y. He and K. T. Law, Superconducting orbital magnetoelectric effect and its evolution across the superconductor-

normal metal phase transition, Phys. Rev. Res. **3**, L032012 (2021).

[48] L. Chirolli, M. T. Mercaldo, C. Guarcello, F. Giazotto, and M. Cuoco, Colossal Orbital Edelstein Effect in Noncentrosymmetric Superconductors, Phys. Rev. Lett. **128**, 217703 (2022).

[49] C. Xiao, H. Liu, J. Zhao, S. A. Yang, and Q. Niu, Thermoelectric generation of orbital magnetization in metals, Phys. Rev. B **103**, 045401 (2021).

[50] C. Xiao, Y. Ren, and B. Xiong, Adiabatically induced orbital magnetization, Phys. Rev. B **103**, 115432 (2021).

[51] K. Shinada, A. Kofuji, and R. Peters, Quantum theory of the intrinsic orbital magnetoelectric effect in itinerant electron systems at finite temperatures, Phys. Rev. B **107**, 094106 (2023).

[52] T. P. Cysne, F. S. M. Guimarães, L. M. Canonico, T. G. Rappoport, and R. B. Muniz, Orbital magnetoelectric effect in zigzag nanoribbons of *p*-band systems, Phys. Rev. B **104**, 165403 (2021).

[53] T. P. Cysne, F. S. M. Guimarães, L. M. Canonico, M. Costa, T. G. Rappoport, and R. B. Muniz, Orbital magnetoelectric effect in nanoribbons of transition metal dichalcogenides, Phys. Rev. B **107**, 115402 (2023).

[54] C. M. Wang and M. Q. Pang, Thermally induced spin polarization and thermal conductivities in a spin-orbit-coupled two-dimensional electron gas, Solid State Commun. **150**, 1509 (2010).

[55] A. Dyrdał, M. Inglot, V. K. Dugaev, and J. Barnaś, Thermally induced spin polarization of a two-dimensional electron gas, Phys. Rev. B **87**, 245309 (2013).

[56] C. Xiao, D. Li, and Z. Ma, Thermoelectric response of spin polarization in rashba spintronic systems, Front. Phys. **11**, 117201 (2016).

[57] A. Dyrdał, J. Barnaś, V. K. Dugaev, and J. Berakdar, Thermally induced spin polarization in a magnetized two-dimensional electron gas with Rashba spin-orbit interaction, Phys. Rev. B **98**, 075307 (2018).

[58] A. Shitade, A. Daido, and Y. Yanase, Theory of spin magnetic quadrupole moment and temperature-gradient-induced magnetization, Phys. Rev. B **99**, 024404 (2019).

[59] L. Smrcka and P. Streda, Transport coefficients in strong magnetic fields, J. Phys. C: Solid State Phys. **10**, 2153 (1977).

[60] T. Qin, Q. Niu, and J. Shi, Energy Magnetization and the Thermal Hall Effect, Phys. Rev. Lett. **107**, 236601 (2011).

[61] J. M. Luttinger, Theory of thermal transport coefficients, Phys. Rev. **135**, A1505 (1964).

[62] As seen in the following discussion and in Appendix A, the order of the limits does not affect the interband case; however, it affects the intraband case. The system is always in equilibrium under a temperature gradient in the static limit ($q \to 0$ before $\omega \to 0$). On the other hand, for the uniform limit ($q \to 0$ after $\omega \to 0$), the system is driven by a temperature gradient to a nonequilibrium state. In this paper, we focus on the latter limit.

[63] A. Shitade, H. Watanabe, and Y. Yanase, Theory of orbital magnetic quadrupole moment and magnetoelectric susceptibility, Phys. Rev. B **98**, 020407(R) (2018).

[64] Y. Gao, D. Vanderbilt, and D. Xiao, Microscopic theory of spin toroidization in periodic crystals, Phys. Rev. B **97**, 134423 (2018).

[65] Y. Gao and D. Xiao, Orbital magnetic quadrupole moment and nonlinear anomalous thermoelectric transport, Phys. Rev. B **98**, 060402(R) (2018).

[66] A. Shitade and Y. Yanase, Magnon gravitomagnetoelectric effect in noncentrosymmetric antiferromagnetic insulators, Phys. Rev. B **100**, 224416 (2019).

[67] R. Winkler and U. Zülicke, Collinear orbital antiferromagnetic order and magnetoelectricity in quasi-two-dimensional itinerant-electron paramagnets, ferromagnets, and antiferromagnets, Phys. Rev. Res. **2**, 043060 (2020).

[68] A. Shitade and G. Tatara, Spin accumulation without spin current, Phys. Rev. B **105**, L201202 (2022).

[69] J. P. Provost and G. Vallee, Riemannian structure on manifolds of quantum states, Commun. Math. Phys. **76**, 289 (1980).

[70] R. Resta, The insulating state of matter: A geometrical theory, Eur. Phys. J. B **79**, 121 (2011).

[71] I. Souza, T. Wilkens, and R. M. Martin, Polarization and localization in insulators: Generating function approach, Phys. Rev. B **62**, 1666 (2000).

[72] A. Daido, A. Shitade, and Y. Yanase, Thermodynamic approach to electric quadrupole moments, Phys. Rev. B **102**, 235149 (2020).

[73] S. Peotta and P. Törmä, Superfluidity in topologically nontrivial flat bands, Nat. Commun. **6**, 8944 (2015).

[74] H. Watanabe and Y. Yanase, Chiral Photocurrent in Parity-Violating Magnet and Enhanced Response in Topological Antiferromagnet, Phys. Rev. X **11**, 011001 (2021).

[75] J. Ahn, G.-Y. Guo, and N. Nagaosa, Low-Frequency Divergence and Quantum Geometry of the Bulk Photovoltaic Effect in Topological Semimetals, Phys. Rev. X **10**, 041041 (2020).

[76] J. Ahn, G.-Y. Guo, N. Nagaosa, and A. Vishwanath, Riemannian geometry of resonant optical responses, Nat. Phys. **18**, 290 (2022).

[77] P. Bhalla, K. Das, D. Culcer, and A. Agarwal, Resonant Second-Harmonic Generation as a Probe of Quantum Geometry, Phys. Rev. Lett. **129**, 227401 (2022).

[78] Y. Gao and D. Xiao, Nonreciprocal Directional Dichroism Induced by the Quantum Metric Dipole, Phys. Rev. Lett. **122**, 227402 (2019).

[79] N. F. Mott and H. Jones, *The Theory of the Properties of Metals and Alloys*, International Series of Monographs on Physics (Clarendon, Oxford, 1936).

[80] D. Xiao, Y. Yao, Z. Fang, and Q. Niu, Berry-Phase Effect in Anomalous Thermoelectric Transport, Phys. Rev. Lett. **97**, 026603 (2006).

[81] C. Xiao, J. Zhu, B. Xiong, and Q. Niu, Conserved spin current for the mott relation, Phys. Rev. B **98**, 081401(R) (2018).

[82] L. Dong, C. Xiao, B. Xiong, and Q. Niu, Berry Phase Effects in Dipole Density and the Mott Relation, Phys. Rev. Lett. **124**, 066601 (2020).

[83] M. I. Aroyo, J. M. Perez-Mato, C. Capillas, E. Kroumova, S. Ivantchev, G. Madariaga, A. Kirov, and H. Wondratschek, Bilbao crystallographic server: I. databases and crystallographic computing programs, Zeitschrift für Kristallographie-Crystalline Materials **221**, 15 (2006).

[84] M. I. Aroyo, A. Kirov, C. Capillas, J. M. Perez-Mato, and H. Wondratschek, Bilbao crystallographic server. ii. representations of crystallographic point groups and space groups, Acta Crystallogr., Sect. A: Found Crystallogr. **62**, 115 (2006).

[85] M. I. Aroyo, J. M. Perez-Mato, D. Orobengoa, E. Tasci, G. de la Flor, and A. Kirov, Crystallography online: Bilbao crystallographic server, Bulg. Chem. Commun **43**, 183 (2011).

[86] I. Sodemann and L. Fu, Quantum Nonlinear Hall Effect Induced by Berry Curvature Dipole in Time-Reversal Invariant Materials, Phys. Rev. Lett. **115**, 216806 (2015).

[87] C. Wang, Y. Gao, and D. Xiao, Intrinsic Nonlinear Hall Effect in Antiferromagnetic Tetragonal CuMnAs, Phys. Rev. Lett. **127**, 277201 (2021).

[88] H. Liu, J. Zhao, Y.-X. Huang, W. Wu, X.-L. Sheng, C. Xiao, and S. A. Yang, Intrinsic Second-Order Anomalous Hall Effect and Its Application in Compensated Antiferromagnets, Phys. Rev. Lett. **127**, 277202 (2021).

[89] K. Ota, M. Shimozawa, T. Muroya, T. Miyamoto, S. Hosoi, A. Nakamura, Y. Homma, F. Honda, D. Aoki, and K. Izawa, Zero-field current-induced hall effect in ferrotoroidic metal, arXiv:2205.05555.

[90] H. Saito, K. Uenishi, N. Miura, C. Tabata, H. Hidaka, T. Yanagisawa, and H. Amitsuka, Evidence of a new current-induced magnetoelectric effect in a toroidal magnetic ordered state of UNi_4B, J. Phys. Soc. Jpn. **87**, 033702 (2018).

[91] C. M. Varma, Non-fermi-liquid states and pairing instability of a general model of copper oxide metals, Phys. Rev. B **55**, 14554 (1997).

[92] B. Fauqué, Y. Sidis, V. Hinkov, S. Pailhès, C. T. Lin, X. Chaud, and P. Bourges, Magnetic Order in the Pseudogap Phase of High-T_C Superconductors, Phys. Rev. Lett. **96**, 197001 (2006).

[93] Y. Li, V. Balédent, N. Barišić, Y. Cho, B. Fauqué, Y. Sidis, G. Yu, X. Zhao, P. Bourges, and M. Greven, Unusual magnetic order in the pseudogap region of the superconductor $HgBa_2CuO_{4+\delta}$, Nature (London) **455**, 372 (2008).

[94] S. S. Pershoguba, K. Kechedzhi, and V. M. Yakovenko, Proposed Chiral Texture of the Magnetic Moments of Unit-Cell Loop Currents in the Pseudogap Phase of Cuprate Superconductors, Phys. Rev. Lett. **111**, 047005 (2013).

[95] L. Zhao, C. A. Belvin, R. Liang, D. A. Bonn, W. N. Hardy, N. P. Armitage, and D. Hsieh, A global inversion-symmetry-broken phase inside the pseudogap region of $YBa_2Cu_3O_y$, Nat. Phys. **13**, 250 (2017).

[96] P. Bourges and Y. Sidis, Novel magnetic order in the pseudogap state of high-tc copper oxides superconductors, C. R. Phys. **12**, 461 (2011).

[97] P. Bourges, D. Bounoua, and Y. Sidis, Loop currents in quantum matter, C.s R. Phys. **22**, 7 (2021).

[98] Y.-X. Jiang, J.-X. Yin, M. M. Denner, N. Shumiya, B. R. Ortiz, G. Xu, Z. Guguchia, J. He, Md. S. Hossain, X. Liu *et al.*, Unconventional chiral charge order in kagome superconductor KV_3Sb_5, Nature Mater. **20**, 1353 (2021).

[99] C. Mielke, D. Das, J.-X. Yin, H. Liu, R. Gupta, Y.-X. Jiang, M. Medarde, X. Wu, H. C. Lei, J. Chang *et al.*, Time-reversal symmetry-breaking charge order in a kagome superconductor, Nature (London) **602**, 245 (2022).

[100] H. Murayama, K. Ishida, R. Kurihara, T. Ono, Y. Sato, Y. Kasahara, H. Watanabe, Y. Yanase, G. Cao, Y. Mizukami, T. Shibauchi, Y. Matsuda, and S. Kasahara, Bond Directional Anapole Order in a Spin-Orbit Coupled Mott Insulator $Sr_2(Ir_{1-x}Rh_x)O_4$, Phys. Rev. X **11**, 011021 (2021).

[101] L. Zhao, D. H. Torchinsky, H. Chu, V. Ivanov, R. Lifshitz, R. Flint, T. Qi, G. Cao, and D. Hsieh, Evidence of an odd-parity hidden order in a spin–orbit coupled correlated iridate, Nat. Phys. **12**, 32 (2016).

[102] J. Jeong, Y. Sidis, A. Louat, V. Brouet, and P. Bourges, Time-reversal symmetry breaking hidden order in $Sr_2(Ir, Rh)O_4$, Nat. Commun. **8**, 1 (2017).

[103] R. Fittipaldi, R. Hartmann, M. T. Mercaldo, S. Komori, A. Bjørlig, W. Kyung, Y. Yasui, T. Miyoshi, L. A. B. Olde Olthof, C. M. Palomares Garcia *et al.*, Unveiling unconventional magnetism at the surface of Sr_2RuO_4, Nat. Commun. **12**, 5792 (2021).

[104] J. Liu, Z. Ma, J. Gao, and X. Dai, Quantum Valley Hall Effect, Orbital Magnetism, and Anomalous Hall Effect in Twisted Multilayer Graphene Systems, Phys. Rev. X **9**, 031021 (2019).

[105] J. Liu and X. Dai, Theories for the correlated insulating states and quantum anomalous hall effect phenomena in twisted bilayer graphene, Phys. Rev. B **103**, 035427 (2021).

[106] N. Bultinck, E. Khalaf, S. Liu, S. Chatterjee, A. Vishwanath, and M. P. Zaletel, Ground State and Hidden Symmetry of Magic-Angle Graphene at Even Integer Filling, Phys. Rev. X **10**, 031034 (2020).

[107] J. Liu and X. Dai, Orbital magnetic states in moiré graphene systems, Nat. Rev. Phys. **3**, 367 (2021).

[108] Y. He, J. Moore, and C. M. Varma, Berry phase and anomalous hall effect in a three-orbital tight-binding hamiltonian, Phys. Rev. B **85**, 155106 (2012).